International Immunopharmacology 66 (2019) 205–214

Contents lists available at ScienceDirect

International Immunopharmacology

journal homepage: www.elsevier.com/locate/intimp

Mce-associated protein Rv0177 alters the cell wall structure of *Mycobacterium smegmatis* and promotes macrophage apoptosis via regulating the cytokines

Shuangquan Yan[1], Junfeng Zhen[1], Yue Li, Chenhui Zhang, Andrea Stojkoska, Nzungize Lambert, Qiming Li, Ping Li, Jianping Xie[*]

Institute of Modern Biopharmaceuticals, State Key Laboratory Breeding Base of Eco-Environment and Bio-Resource of the Three Gorges Area, Key Laboratory of Ministry of Education Eco-Environment of the Three Gorges Reservoir Region, School of Life Sciences, Southwest University, Chongqing 400715, China

ARTICLE INFO

Keywords:
Mycobacterium tuberculosis
Rv0177
Cytokines
Apoptosis
Endoplasmic reticulum stress

ABSTRACT

The success of *Mycobacterium tuberculosis* as a pathogen largely contributes to its ability to infect, modify and persist within the host cells. *M. tuberculosis Rv0177* is a gene of the *mce1* operon (Mammalian cell entry), encoding a conserved hypothetical protein, essential for *M. tuberculosis* survival and up-regulated within murine macrophages. To explore its function, *Rv0177* was heterologously expressed in *M. smegmatis*. The recombinant protein was located in the cell wall. *M. smegmatis* recombinant strain expressing Rv0177 altered sliding motility, its cell wall architecture and the permeability. Moreover, *M. smegmatis* expressing Rv0177 could up-regulate MCP-1 and downregulate the IL-6 expression in RAW264.7 macrophages in comparison to the control. MS_Rv0177 increased the expression of MCP-1 inducible protein (MCPIP) and a C/EBP homologous protein (CHOP) owing to MCP-1. In addition, the JNK signaling pathway was engaged in the interplay between MS_Rv0177 and macrophages. The macrophage caspase-3 activation and cell apoptosis were induced by the recombinant. This provided novel functional cues for the MCE-associated Rv0177.

1. Introduction

Tuberculosis (TB) caused by *Mycobacterium tuberculosis* remains a formidable threat to the global public health with millions of deaths and around 9 million of infections each year [1]. *M. tuberculosis* virulence factors have been extensively characterized [2–6]. However, the roles of the *mce* operons still remain elusive although several mce proteins are reported to be involved in the pathogenesis of *M. tuberculosis*.

M. tuberculosis H37Rv genome has *mce*1–4 operons, each including two *yrbE* genes (*yrbEA* and *yrbEB*) and six *mce* genes (*mceA*, *mceB*, *mceC*, *mceD*, *mceE* and *mceF*) [7,8]. The *mce*1–4 operons encode ABC-like transporter is important for the lipid homeostasis of *M. tuberculosis* [9]. The *mce4* encodes a cholesterol import system, essential for *M. tuberculosis* to persist within IFN-γ activated macrophages and in the lungs of animals during chronic infection [10]. The recombinant LprN protein of *mce*4 operon can increase the production of TNF-α and IFN-γ to induce Th-1 type response in the BALB/c mice [11]. The Mce3E protein of *mce*3 operon suppressed the expression of TNF-α and IL-6 via reducing the phosphorylation and inhibiting the translocation of ERK 1/2 in RAW 264.7 murine macrophages [12]. *M. bovis* mce2-phoP double knockout as candidate vaccine against the *M. bovis* [13]. 13 genes (*Rv0166-Rv0178*) of *mce*1 operon were co-transcribed and negatively regulated by *Mce1R* (*Rv0165*) in vivo [14,15]. Fatty-acyl-CoA synthetase FadD5 is crucial for the metabolism of mycolic acid [16]. Polystyrene latex microspheres coated with the purified recombinant Mce1A (Rv0167) protein are more readily uptake by HeLa cells [17]. The disruption of *mce*1 operon resulted in accumulation of free mycolates (mainly alpha, methoxy and keto mycolates) in the cell wall [18–20]. The hypervirulent mutant reduced the cellular production of TNF-α, IL-6 and nitric oxide (NO) through the Toll-like receptor 2 [21–24].

Rv0177 is one of the 54 predicted proteins involved in the host-pathogen interaction [25]. To explore its roles, the Rv0177 recombinant *M. smegmatis* was constructed. The results show that the *Rv0177* gene could alter the cytokines profile of the RAW264.7 murine macrophages, and induce cell apoptosis.

[*] Corresponding author.
E-mail address: georgex@swu.edu.cn (J. Xie).
[1] These authors equally contributed to the work.

https://doi.org/10.1016/j.intimp.2018.11.013
Received 16 May 2018; Received in revised form 26 October 2018; Accepted 9 November 2018
Available online 22 November 2018

Table 1
The primers used in this study.

Primers	Sequences (5′-3′)
pNIT-Rv0177 -For	GAATTCATGAGCCCCCGTCGTAAGTTTG
pNIT-Rv0177 -Rev	GCATGCGATCACCGGAAGCAGACTG
MCP-1-For	CTTCTGGGCCTGCTGTTCA
MCP-1-Rev	CCAGCCTACTCATTGGGATCA
IL-6 -For	CTGCAAGAGACTTCCATCCAG
IL-6- Rev	AGTGGTATAGACAGGTCTGTTGG
MCPIP-For	CCCCCTGACGACCCTTTAG
MCPIP-Rev	GGCAGTGGTTTCTTACGAAGGA
CHOP-For	CATCACCTCCTGTCTGTCTC
CHOP-Rev	AGCCCTCTCCTGGTCTAC
GRP78-For	AGGATGCGGACATTGAAGAC
GRP78-Rev	AGGTGAAGATTCCAATTACATTCG
β-actin-For	AGAGGGAAATCGTGCGTGAC
β-actin-Rev	CAATAGTGATGACCTGGCCGT

2. Materials and methods

2.1. Bacterial strains, plasmids and culture conditions

Escherichia coli DH5α and *Mycobacterium smegmatis* mc^2 155 strains were preserved by the Institute of Modern Biopharmaceuticals. We used pNIT-Myc plasmid (*Mycobacterium* shuttle vector) constructed from pNIT-1 harboring a Myc-tag for Western blotting [26]. *M. smegmatis* mc^2 155 was grown in Middlebrook (MB) 7H9 liquid medium supplemented with 0.05% (v/v) Tween 80, 0.5% (v/v) glycerol and 0.2% (w/v) glucose or Middlebrook (MB) 7H10 agar plates. When necessary, the culture media were supplemented with the antibiotic kanamycin (25 μg/ml for *Mycobacterium* and 50 μg/ml for *E. coli*) and ampicillin (50 μg/ml).

2.2. Construction of recombinant M. smegmatis expressing Rv0177

The primers used in our study are listed in Table 1. The full-length of the gene was amplified by PCR using the gene-specific primers from the *M. tuberculosis* H37Rv genome. The PCR fragments were digested by *Eco*RI and *Sph*I, then purified and ligated into the modified pNIT-Myc shuttle vector. The plasmids (pNIT-*Rv0177*-Myc and pNIT-Myc) were electroporated into the nonpathogenic *M. smegmatis* mc^2 155, respectively. The recombinant strain colonies were selected on MB 7H10 agar plates containing the antibiotic kanamycin (25 μg/ml). The successfully transformed constructs were further confirmed by PCR amplification. The recombinant *M. smegmatis* strains harbored pNIT_Rv0177_Myc or pNIT_Myc vector was grown in MB 7H9 medium supplemented with 25 μg/ml kanamycin and 28 mM ε-caprolactam inducer (Aladdin, China). After induction, the bacterial pellets were harvested and sonicated. The samples were subjected to SDS-PAGE and further detected by Western blotting with the anti-Myc antibody (TIANGEN, China). The blots were formed after incubation with the secondary antibody, a goat anti-mouse IgG-HRP monoclonal antibody labeled with horseradish peroxidase (TIANGEN, China).

2.3. Subcellular localization of Rv0177 protein in M. smegmatis

Subcellular localization of the Rv0177 protein was identified by using the methods previously reported [27,28]. Briefly, the MS_Rv0177 and MS_Vec were grown to OD_{600} = 0.6–0.8, adding 28 mM ε-caprolactam for 16 h induction. Bacterial cell pellets were harvested and sonicated, then the whole lysates were centrifuged at 3000 ×*g* for 5 min at 4 °C to separate the intact cells and cell debris. The supernatant was centrifuged at 27,000 ×*g* for 40 min at 4 °C, the cell wall fraction, cell membrane and cytoplasmic fraction were collected separately, followed by SDS-PAGE and Western blotting to determine the expression and location of the Rv0177 protein. GroEL2 was a cytoplasmic control from native *M. smegmatis* containing an endogenous histidine. The anti-His tag antibody (TIANGEN, China) was used for the assay [29].

2.4. Sliding motility measurement

For the sliding motility assay, 7H9 media supplemented with 0.3% agarose was prepared. Then 3 μl of cell culture at an OD_{600} of 0.4 with ten-fold serial dilutions was carefully spotted onto the center of the plates. The scale of cell motility was measured after 5–6 days.

2.5. Transmission electron microscopy (TEM)

For TEM, MS_Rv0177 and MS_Vec were induced, washed and collected at 4000 ×g for 10 min. The bacterial cells were separated gently, continuously centrifuged at 1000 ×*g* for 15 min and then fixed with 4% glutaraldehyde for 2 h at 4 °C. Ultra-thin sections (50–70 nm) were made with a glass knife on ultra-microtome. Specimens were examined by the H-7500 transmission electron microscopy (Hitachi).

2.6. Permeability assay

The ethidium bromide (EB), low molecular fluorescent dye, can readily penetrate the bacterial cells. The induced recombinant strains were washed with 1× PBS containing 0.05% Tween80 (PBST). The bacterial cells were stained with 2 μg/ml EB (Sigma) in 96-well plates. The plates were read by excitation at 544 nm and emission at 590 nm at an interval of 5 min for 1 h on a microplate reader (BMG Labtech) to determine the fluorescence intensity of intracellular EB. The mean value from three independent repeats.

2.7. Intracellular survival

RAW264.7 macrophages were cultured in RPMI-1640 medium containing 10% heat-inactivated fetal bovine serum (FBS), 100 U/ml penicillin, 100 μg/ml streptomycin (Invitrogen) and 2 mM glutamine. Then RAW264.7 macrophages were maintained in a humidified incubator supplemented with 5% CO_2 at 37 °C.

RAW264.7 cells were seeded at 1×10^6 per well in 12-well tissue culture plates. After 18 h, the macrophages were infected with MS_Rv0177 and MS_Vec at a multiplicity of infection (MOI) of 10:1. After 4 h of infection, cells were washed three times with sterilized 1× PBS, then fresh RPMI-1640 medium was added containing 10% FBS supplemented with 250 nM IVN (Sigma) dissolved in DMSO and 100 μg/ml hygromycin B (Roche, USA). After 6 h, 24 h, 48 h and 72 h of infection, cells were washed three times and lysed with sterilized 0.025% (w/v) SDS in water. The lysed macrophages were spotted on the MB 7H10 plates at ten-fold dilution and colonies were enumerated after 3–4 days at 37 °C.

2.8. Cell viability and cell cytotoxicity

RAW264.7 cells were plated in the 96-well plates. The cells were infected with the recombinant strains and collected at different time 6 h, 24 h, and 48 h after infection, the samples were harvested and 10 μl MTT (3-(4-5-dimethylthiazol-2-yl)-2,5-diphenyl tetrazolium bromide, 5 mg/ml) was added to each well and incubated for 3 h at 37 °C. The intracellular accumulated formazan from the reduced MTT was dissolved by DMSO and measured at 570 nm on the microplate reader.

RAW264.7 cells were seeded at 1×10^6 per well in 12-well tissue culture plates. The macrophages were infected with MS_Vec and MS_Rv0177 at MOI = 10:1 and the culture supernatants were collected at 6 h and 24 h. The release lactate dehydrogenase (LDH) activity of RAW264.7 macrophages was measured with the Cytotox96 Cytotoxicity Assay Kit (Promega, USA) to evaluate the cytotoxicity [30].

2.9. Apoptosis analysis

The apoptotic cells were detected using the Annexin V-FITC/PI Apoptosis Detection Kit (Shanghai, PR China). The cells were washed with sterilized 1× PBS buffer three times and stained with 10 μl Annexin V-FITC and 5 μl propidium iodide (PI) for 10 min at 37 °C in the dark. The stained cells were observed using a fluorescence microscope.

2.10. Assay for cytokine production

Total RNA was collected with the bacterial/cell RNA extraction kit (TIANGEN, China) according to the manufacturer's instructions. The DNAase treated total RNA (1 μg) was transcribed into cDNA and quantitative RT-PCR was performed with the indicated primers for β-actin, MCP-1, IL-6, MCPIP, GRP78 and CHOP genes (Table 1). Then the concentration of cytokines in the infected RAW264.7 cells supernatant was determined by the ELISA kits for MCP-1 and IL-6 as the manufacturer's protocols (Shanghai, China).

2.11. Statistical analysis

The data was analyzed using Student's two-tailed *t*-test. Significance was defined as P values (*P < 0.05, **P < 0.01, ***P < 0.001, ns = not significant). Error bars represent standard deviation.

3. Results

3.1. M. tuberculosis Rv0177 can be heterologously expressed in M. smegmatis

Rv0177 is a member of *mce*1 operon conserved among *M. tuberculosis*, *M. bovis*, *M. leprae*, *M. marinum* and non-pathogenic *M. smegmatis* (Fig. S1). The 555 bp *M. tuberculosis Rv0177* gene encodes a 20 kDa protein. In our study, two recombinant *M. smegmatis* strains were constructed. The MS_Rv0177 strain harbored the recombinant pNIT_*Rv0177*_Myc vector, while the MS_Vec only harbored pNIT_Myc. Both MS_Rv0177 and MS_Vec, were grown in 7H9 medium supplemented with kanamycin. The PCR product of *Rv0177* gene was confirmed (Fig. 1A). The 25 kDa Rv0177_Myc fusion protein was identified by Western blotting but it was absent in MS_Vec (Fig. 1B).

3.2. Rv0177 protein is cell wall localized in the recombinant strain

Rv0177 protein is highly conserved in mycobacterial strains with a predicted transmembrane domain in bioinformatics. To determine its subcellular location, the induced MS_Vec and MS_Rv0177 bacterial pellets were sonicated, fractioned and subjected to Western blotting. The data showed that Rv0177 protein was exclusively present in the cell wall fraction while absent in the cytoplasmic and membrane fraction. The control heat-shock protein GroEL2 was present in the *M.*

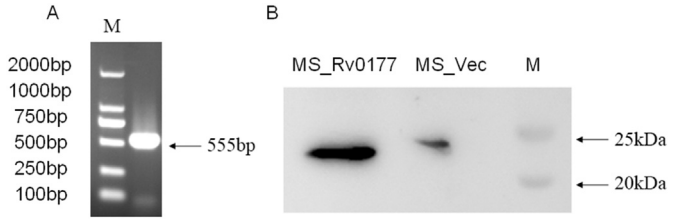

Fig. 1. Overexpression of Rv0177 in recombinant *M. smegmatis*. (A) The colony bacteria PCR amplification of the recombinant strains using the design primers. (B) Lysates were prepared from the bacterial cells and subjected to Western blotting analysis to detect the Myc-tag Rv0177 fusion protein by using the mouse anti-Myc antibody.

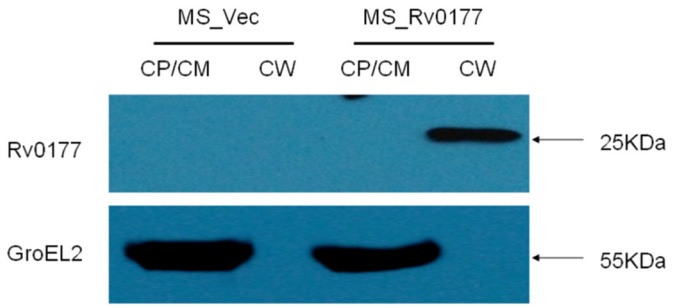

Fig. 2. Rv0177 protein is associated with *Mycobacterium* cell wall. The recombinant strain of *M. smegmatis* was induced to express Rv0177 protein localized in the cell wall fractions. Subcellular fractions were separated by SDS-PAGE and Rv0177 was detected with an anti-Myc antibody. GroEL2 was detected with an anti-His antibody as a cytoplasmic control of *M. smegmatis*. CP/CM (cell cytoplasm and cell membrane fraction), CW (cell wall fraction).

smegmatis cytoplasm (Fig. 2).

3.3. The Rv0177 recombinant shows altered sliding mobility

In relation to the pathogenesis of *M. tuberculosis*, we detected the sliding behavior to explore the physiological effect of *Rv0177*. The increased sliding motility on the 7H9 plate supplemented with 0.3% agarose was observed for the Rv0177 recombinants (Fig. 3). According to the previous reports, sliding mobility of mycobacteria was closely associated with an alteration in the profile of glycopeptidolipids (GPLs) and mycolic acids within the mycobacterial cell wall [31,32]. We performed cell wall lipid analysis, however, overexpression of Rv0177 protein did not significantly affect the fatty acid compositions and GPLs detected by GC–MS assay (Fig. S2) and TLC analysis (data not shown), respectively.

3.4. Rv0177 protein expression alters cell wall structure and decreases its permeability

To further explore the alterations of the cell wall architecture, we performed the transmission electron microscopy (TEM) analysis. MS_Vec recombinant showed indistinct cell wall surface (Fig. 4Aa, b), while MS_Rv0177 recombinant cell wall was more compact (Fig. 4Ac, d), consistent with the divergent sliding motility in both recombinants. Ethidium bromide (EB) is a small diffusible fluorescence dye; it could penetrate into the bacterial cell wall and membrane freely. The EB uptake assay was performed to check the cell wall permeability. As the result, the accumulation of the intracellular EB of MS_Rv0177 was significantly lower than MS_Vec after 1-hour treatment (Fig. 4B). This suggests that the overexpression of Rv0177 significantly decreased the cell envelope permeability, which further confirmed that the cell wall localization of Rv0177 altered the cell wall architecture in *M. smegmatis*.

3.5. Rv0177 reduces the survival of M. smegmatis in RAW264.7 macrophages

Mce1A-coated polystyrene latex microspheres can be more readily uptaken by non-phagocytic HeLa cells [17]. *M. tuberculosis* Δmce1 mutant is hypervirulent in C57BL/6 mice, with a higher bacterial load in liver, spleen, and lung [21,23]. However, when RAW264.7 macrophages were infected with MS_Rv0177 and MS_Vec for 4 h at a MOI of 20:1, there was no difference in the invasion ability (Fig. 5C). MS_Rv0177 survival within RAW264.7 macrophages at 24 h post-infection is weaker than the MS_Vec (Fig. 5B). In addition, the growth characteristics of MS_Rv0177 and MS_Vec were also similar in the 7H9 medium in vitro (Fig. 5A). Therefore, we speculated that Rv0177

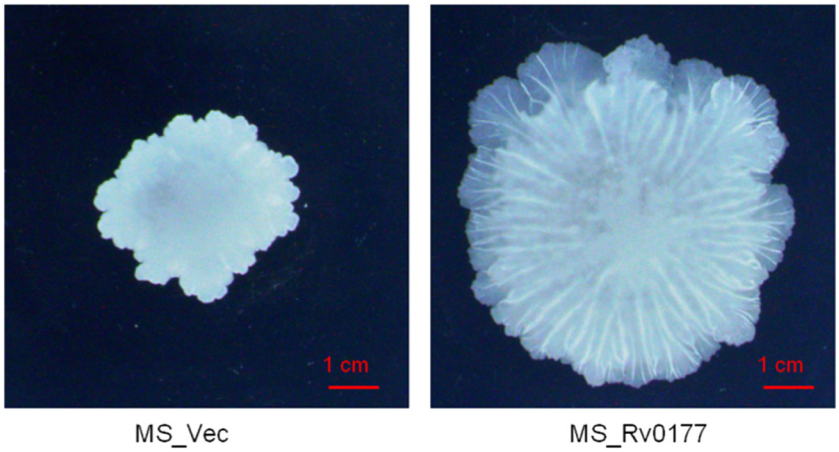

Fig. 3. Assay for the sliding motility for recombinant *M. smegmatis* on 7H9 solid plates supplemented with 0.3% agarose.

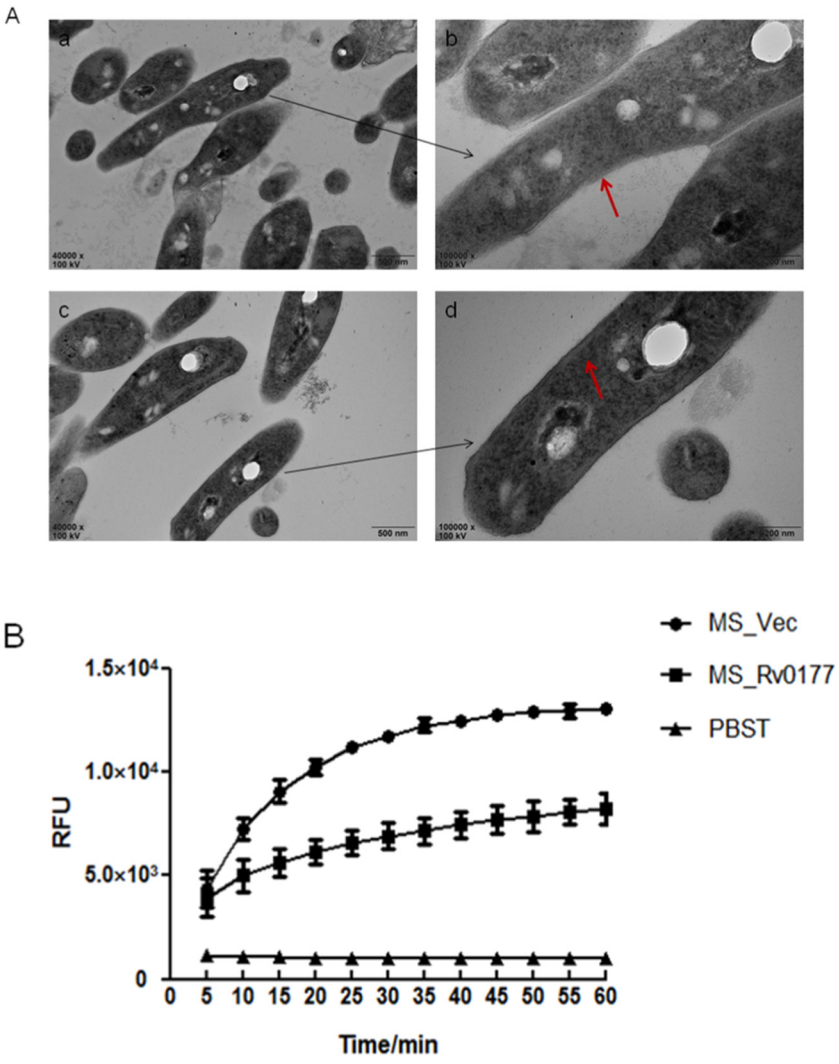

Fig. 4. (A) The transmission electron microscope (TEM) analysis for recombinant *M. smegmatis*. MS_Vec and MS_Rv0177 were grown in the 7H9 medium, collected and fixed by 4% glutaraldehyde for analysis. (a) and (b) were imaged at 40,000× and 100,000× amplification for MS_Vec specimen, respectively; (c) and (d) for MS_Rv0177 specimen. (B) The relative accumulation of the intracellular EB of recombinant *M. smegmatis*. The induced MS_Vec and MS_Rv0177 strains were treated with 2 μg/ml EB and the relative fluorescence units (RFU) of the intracellular EB was measured at an interval of 5 min and consider PBST as a negative control.

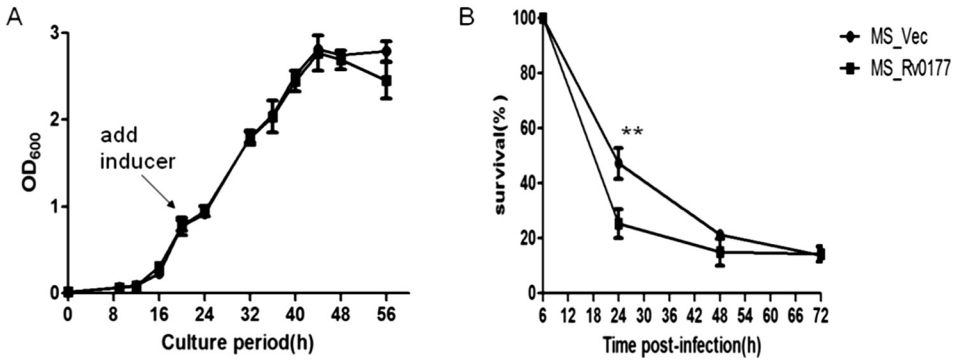

Fig. 5. The intracellular survival of recombinant *M. smegmatis* within macrophages. (A) Growth curve of MS_Vec and MS_Rv0177 at 37 °C in MB 7H9 liquid medium was measured by determining OD_{600} at intervals of 4 h or 8 h. (B) RAW264.7 cells were infected with MS_Vec and MS_Rv0177 as described in the methods section, respectively. (C) The invasion ability of the recombinant strains for RAW264.7 macrophages at a MOI of 20:1 at 4 h post-infection. Invasion ratio represents the ratio of the number of intracellular bacteria and the number of initial infection bacteria. Numbers of intracellular bacteria are shown as a percentage of the numbers recorded at 6 h. Data are shown as means ± SD of triplicate wells. Similar results were obtained in three independent experiments.

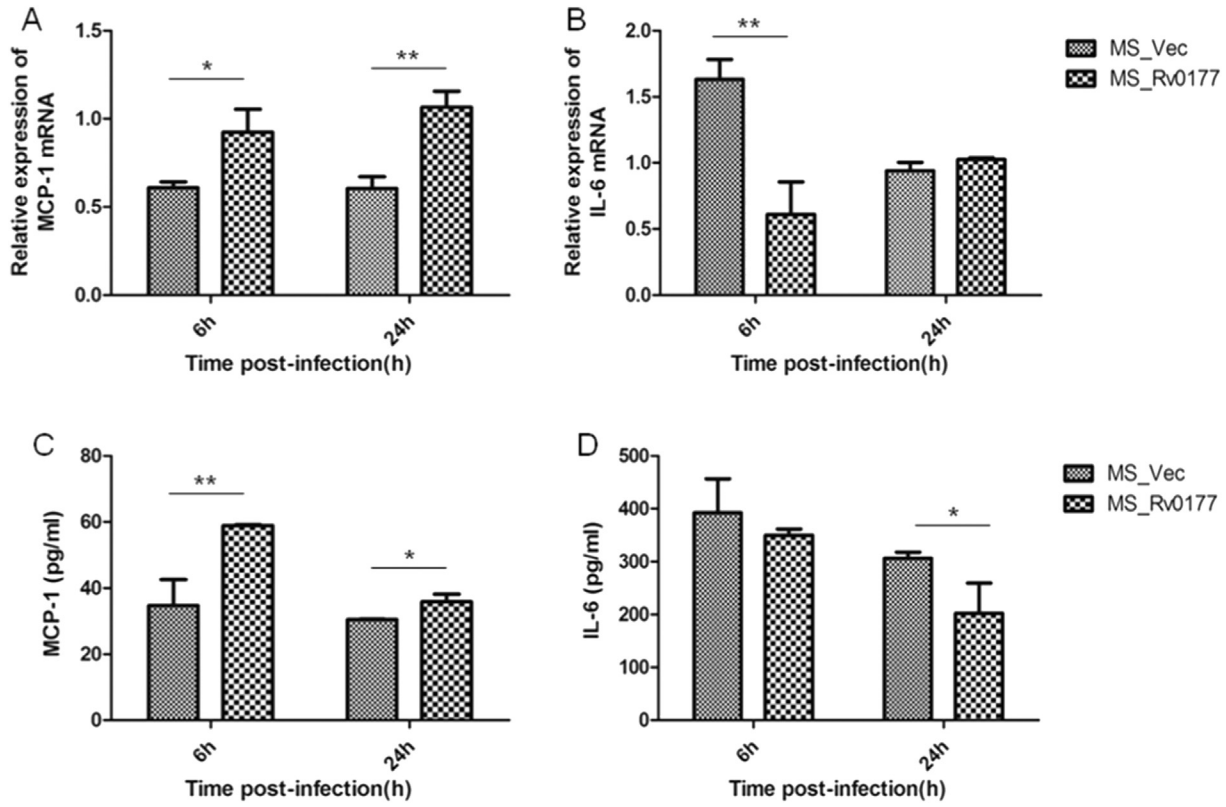

Fig. 6. Rv0177 modifies the expression of cytokines in RAW264.7 macrophages. RAW264.7 were infected with MS_Vec and MS_Rv0177 strains. After 6 and 24 h, the infected macrophages were collected and the expression levels of MCP-1 (A, C) and IL-6 (B, D) were detected by RT-PCR and ELISA. The mRNA level of cytokines was normalized to β-actin mRNA. Similar results were obtained in three independent experiments.

reduces the survival of *M. smegmatis* within macrophages.

3.6. MS_Rv0177 alters the macrophage cytokine profile

To explore the role of *Rv0177* in the virulence of *M. tuberculosis*, RAW264.7 cells were infected with the recombinant *M. smegmatis* strains (MS_Rv0177 and MS_Vec). Transcriptional and translational levels were detected by RT-PCR and ELISA, respectively. Transcriptional levels of TNF-α and IL-1β show no difference. Both transcriptional and expression levels of IL-6 were downregulated in RAW264.7 macrophages infected with MS_Rv0177 (Fig. 6B, D), While Transcriptional and expression level of monocyte chemoattractant protein 1 (MCP-1) was markedly upregulated in comparison to the control MS_Vec (Fig. 6A, C). Both cytokine profiles of MCP-1 and IL-6

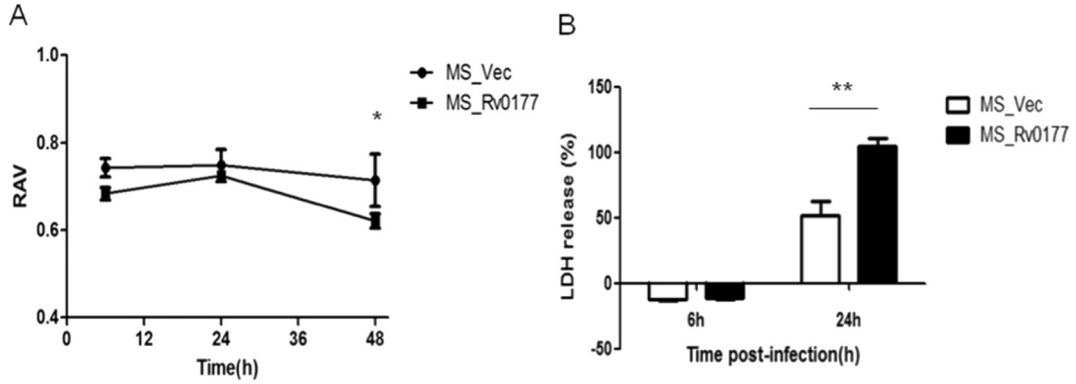

Fig. 7. MS_Rv0177 induces cell death in infected macrophages. (A) The relative absorbance value (RAV) of formazan reduced from MTT in RAW264.7 macrophages was measured at the wavelength of 570 nm by microplate reader. (B) The relative activity of LDH from the supernatant of macrophages death was determined using the Cytotoxicity Assay Kit.

were recapitulated in PMA-differentiated THP-1 cells (data not shown). The data implicated that Rv0177 might tip the balance of cytokines, crucial for the outcome of *Mycobacterium*-host cell interaction.

3.7. MS_Rv0177 affects the viability of macrophages

To determine the potential cytotoxic effect of MS_Rv0177 on macrophages, we tested the viability of RAW264.7 cells infected with recombinant strains using MTT assay after 6 h, 24 h and 48 h post-infection. The results show that the accumulation of formazan from the reduced MTT in MS_Rv0177 infected macrophages was less than MS_Vec at 48 h post-infection (Fig. 7A). Consistently, the relative release LDH activity from the MS_Rv0177 infected macrophages supernatant was higher than MS_Vec at 24 h infection (Fig. 7B). This implicates that MS_Rv0177 was cytotoxic to macrophages.

3.8. MS_Rv0177 promotes macrophages apoptosis

The subverted cytokines tend to trigger cell apoptosis. To study further the role of MS_Rv0177 in cell apoptosis, Annexin V/PI double staining was performed to determine the early and late apoptotic macrophages. The RAW264.7 cells were stained with Annexin V-FITC and PI after 6 h and 48 h of infection. The early apoptotic cells were stained by Annexin V-FITC with the green fluorescence; PI with red fluorescence stained the necrotic cells, while the late apoptotic cells could be stained by both. Comparison of the fluorescence spots in Ms_Rv0177 infected cells and Ms_Vec showed that the percentage of Annexin V-FITC single positive and Annexin V/PI double positive was higher (nearly 1.44 and 1.58 times, respectively) (Fig. 8Ba, b). Western blotting also showed more activation of caspase-3 after 24 h in MS_Rv0177 infected macrophages (Fig. 8A). Taken together, the data indicate that MS_Rv0177 can induce macrophages apoptosis.

3.9. MCPIP and ER stress might be involved in MS_Rv0177-RAW264.7 macrophages interaction

The CCL2/MCP-1 was associated with the establishment and maintenance of granuloma in *M. tuberculosis* latent infection, as well as with the severity of tuberculosis [33,34]. The MCP-1 inducible protein (MCPIP) could be induced through MCP-1 targeting the CCL2 receptor. MCPIP harboring a CCCH-type zinc-finger domain was identified as a novel RNase to cleave the IL-6, IL-12 and itself mRNA [35]. The elevated expression of MCPIP can control the intracellular mycobacteria survival and elicit the ER stress [36,37]. The C/EBP homologous protein (CHOP) is an ER stress molecular chaperone, playing an important role in the ER stress-mediated cell apoptosis [38]. Glucose-regulated protein 78 (GRP78/Bip), another associated ER stress protein, can facilitate the degradation of misfolded proteins to alleviate ER stress [39,40]. To explore whether MS_Rv0177 promotes the expression of MCPIP and induces ER stress, the expression of MCPIP, CHOP and GRP78 were monitored in RAW264.7 macrophages infected with MS_Vec and MS_Rv0177. The infected RAW264.7 cells were collected and lysed for RNA extraction after 6 h and 24 h post-infection, respectively. MCPIP and CHOP transcriptions were upregulated and GRP78 was downregulated in MS_Rv0177 infected macrophages consistent with previous reports [41,42] (Fig. 9). The data suggested that Rv0177 might exert its effect via modulating MCPIP and ER stress.

3.10. JNK signaling pathway is affected by MS_Rv0177

The MAPK signaling pathway (mainly included JNK, p38, and ERK1/2) is involved in the production of MCP-1 and phosphorylated by mycobacterium antigen, which is crucial for the induction of ER stress [36,43,44]. NF-κB, a ubiquitous transcriptional factor, regulates the transcription of a wide spectrum of the immunity-associated genes [45]. To explore whether these factors are engaged in *Rv0177* action, RAW264.7 macrophages were treated with NF-κB inhibitor TPCK, JNK inhibitor SP 600125 and p38 inhibitor SB 202190 for 1 h, respectively, prior to infection with MS_Rv0177 and MS_Vec. The MCP-1 was inhibited by the NF-κB inhibitor in MS_Vec infected macrophages, however, its level was high in MS_Rv0177 infected macrophages. Moreover, the MCP-1 mRNA was significantly inhibited by the JNK inhibitor in MS_Rv0177 infected macrophages, indicating that MS_Rv0177 could effectively modulate the JNK signaling pathway (Fig. 10A). Accordance with that, we checked the reduced transcriptional level of MCPIP and CHOP in MS_Rv0177 infected macrophages for the treatment with the JNK specific inhibitor (Fig. 10B, C). Although the p38 inhibitor could inhibit the expression of MCPIP, the data implicated the JNK signaling participated in MS_Rv0177-mediated ER stress induction and expression of MCP-1and MCPIP.

4. Discussion

Mce-associated Rv0177 protein is essential and up-regulated in murine macrophages [25]. In our study, we established roles of new mce protein in addition to their function in the cell envelope, lipid homeostasis, the invasion and persistence of pathogen into host cells [8,16,20,46,47]. According to the results, *M. smegmatis* recombinant strain expressing Rv0177 altered sliding motility, its cell wall architecture and the permeability. The fatty acidic components (C7–C26) showed no significant divergence. However, further studies are needed to find if a much longer chain of mycolic acids and more complex GPLs of cell wall will show a difference. Cytokines play important roles in the interplay of *M. tuberculosis* and host. MS_Rv0177 modulates the

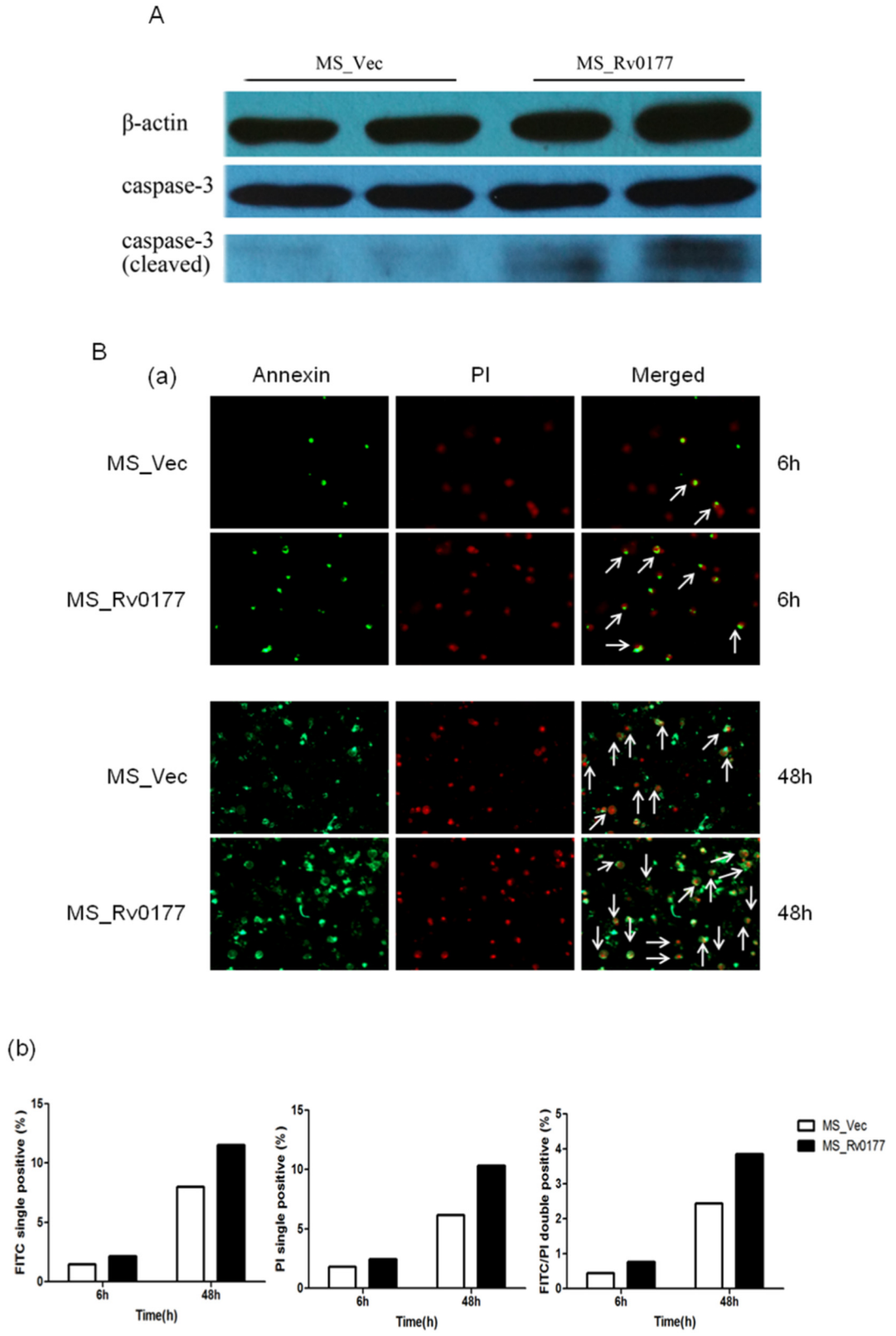

Fig. 8. Microscope images of RAW264.7 macrophages apoptosis infected with the recombinant *M. smegmatis* strains. (A) Western blotting analysis of caspase-3 in RAW264.7 macrophages infected with MS_Rv0177 and MS_Vec for 24 h. (B) (a) the RAW264.7 cells were stained with Annexin V-FITC/PI after the invasion of 6 h and 48 h, and the early (green fluorescence) and late (yellow or red fluorescence) stages of apoptosis were indicated. (b) The proportions of cells undergoing the early (green fluorescence) and late (yellow or red fluorescence) stages of apoptosis were indicated. Data are shown as means ± SM SD of triplicate wells. Similar results were generated by two independent experiments. (For interpretation of the references to colour in this figure legend, the reader is referred to the web version of this article.)

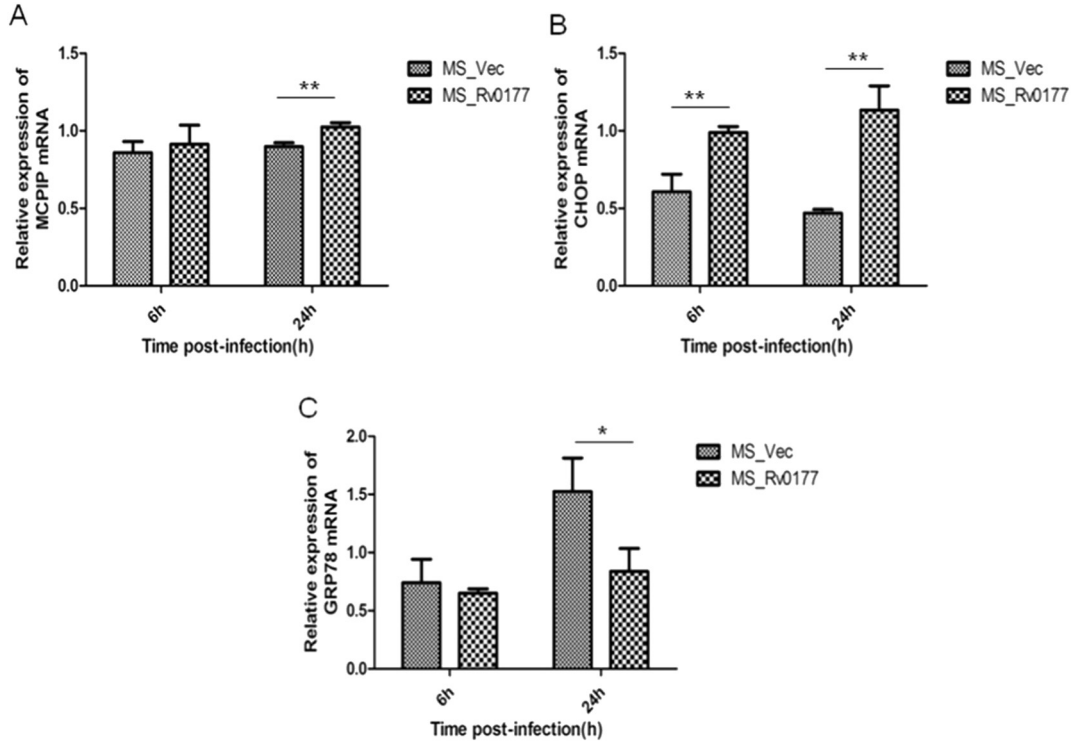

Fig. 9. MS_Rv0177 enhances the expression of MCPIP and induces ER stress in RAW264.7 macrophages. RAW264.7 cells were infected with MS_Vec and MS_Rv0177 strains. After 6 h and 24 h of infection, the infected macrophages were collected and the transcriptional level of MCPIP (A), CHOP (B) and GRP78 (C) were detected by RT-PCR. The mRNA level of MCPIP, CHOP and GRP78 were normalized to that of β-actin mRNA. Similar results were obtained in three independent experiments.

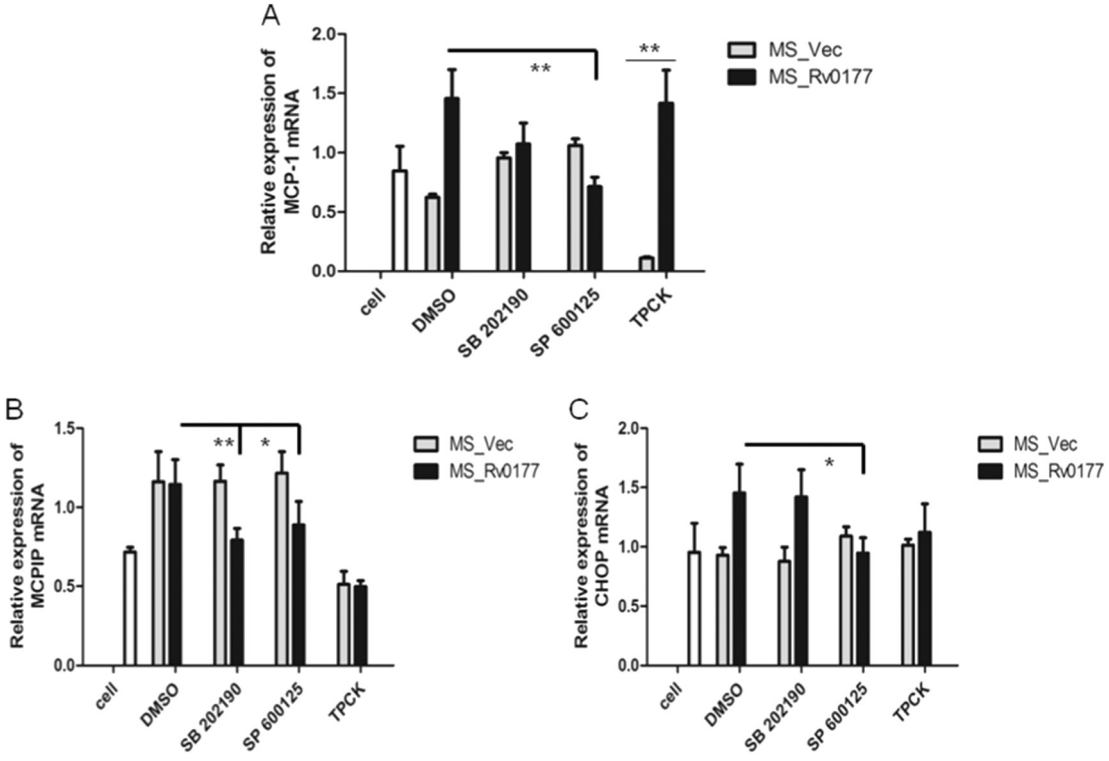

Fig. 10. MS_Rv0177 alters the activation of JNK pathway in macrophages. RAW264.7 cells were pre-treated with 10 μM SB 202190 (a p38 inhibitor), 25 μM SP 600125 (a JNK inhibitor) and 30 μM TPCK (a NF-κB inhibitor). After 1 h, RAW264.7 cells were infected with MS_Rv0177 and MS_Vec at a MOI of 10:1. All cells were collected after 24 h of infection and the transcriptional level of MCP-1 (A), MCPIP (B) and CHOP (C) were detected by RT-PCR. Data were generated from two independent experiments.

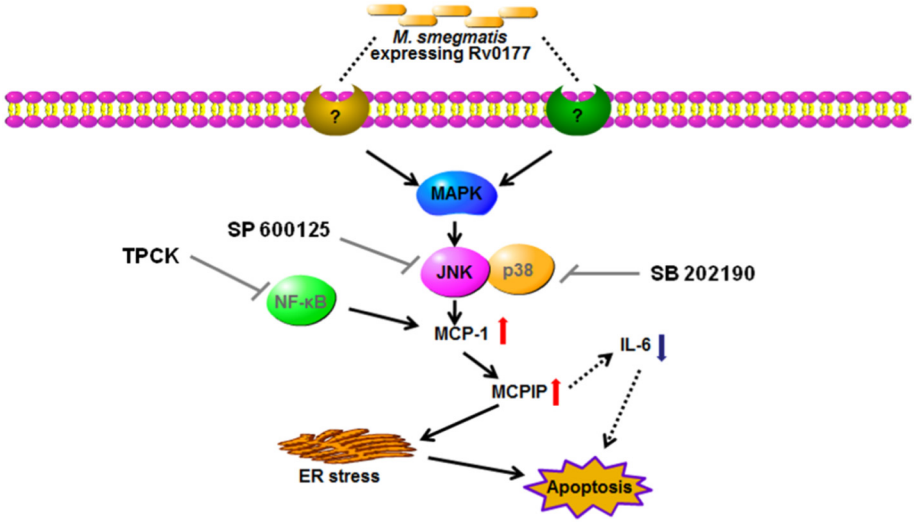

Fig. 11. Proposed model of the recombinant *M. smegmatis* expressing Rv0177 interaction with macrophages. Rv0177 modifies the cytokine profile and results in cell apoptosis, which might be mediated by ER stress via the activation of the JNK pathway. ↑: upregulation; ↓: downregulation. Identified in this study; ---► reported by others. ——| inhibitor treatment of the different signaling pathways. TPCK, a NF-κB inhibitor; SP 600125, a JNK inhibitor; SB 202190, a p38 inhibitor.

cytokine profile of the infected macrophages. IL-6, as a major pro-inflammatory cytokine, is crucial for activating protective Th1 immune responses to kill mycobacterium [48–50]. Other reports proved that the reduced IL-6 production could inhibit the JAK/STAT signaling to induce cell apoptosis [51,52]. In our study, MS_Rv0177 selectively controlled the expression of IL-6 in RAW264.7 macrophages, which might bring apoptosis event of macrophages for this pathogen. CCL-2/MCP-1, a member of the small inducible gene family, is critical in the recruitment of leukocytes to the site of infection [53]. CCL-2/MCP-1 is also important in the establishment of granuloma to maintain the balance of pro-inflammatory and anti-inflammatory [53]. However, the excess of MCP-1 could active Th2 circuit leading to an increased risk of infection and disease progression [33,54]. Its elevated level was related to severe tuberculosis disease [34,55]. It was determined that the expression of MCP-1 was increased in the MS_Rv0177 infected macrophages, but the role of this chemokine in *M. tuberculosis* infection remains to be defined.

MCP-1 can induce monocyte chemotactic protein-induced protein (MCPIP), which would elicit endoplasmic reticulum (ER) stress and further cause cell death and cell apoptosis [41,42,44,56,57]. Based on these studies, we determined that the increased expression of MCPIP and CHOP, as well as the decreased expression of GRP78 in infected RAW264.7 macrophages, can protect the cells from ER stress-induced cell death [39]. Further, when infected macrophages were treated with JNK special inhibitor, the level of MCP-1 was inhibited and expression of MCPIP and CHOP was significantly reduced. We suggested that the production of MCP-1 and the induction of ER stress were associated with the JNK signaling pathway activated by MS_Rv0177.

Macrophages apoptosis could effectively suppress the proliferation of mycobacteria. The caspase proteins are the main molecular markers of cell apoptosis. With Western blotting, we identified the activation of caspase-3. We used Annexin V-FITC/PI assay to determine the induced cell apoptosis in the early and late stage of cell death in MS_Rv0177 infected macrophages. Here, we make the speculation that MS_Rv0177 could increase the level of MCP-1 in macrophages, sequentially induce MCPIP and ER stress-mediated cell apoptosis and cell death via the activation of the JNK signaling pathway (Fig. 11).

Funding

This work was supported by National Natural Science Foundation of China [grant number 81871182, 81371851, 81071316, 81271882,81301394], National Key Research and Development Program (2016YFC0502304), Open Fund of Shanghai Key Laboratory of Tuberculosis (2017-001) the Fundamental Research Funds for the Central Universities [grant numbers XDJK2016E093, XDJK2012D011, XDJK2012D007, XDJK2013D003, XDJK2017D099], The Chongqing Municipal Education Commission for postgraduates innovation program, China [grant numbers CYS16073, CYB18076].

Conflict of interest

All authors declare that they have no conflict of interest.

Ethical approval

No ethical approval is needed for this study.

Informed consent

Informed consent was obtained prior to the study.

Appendix A. Supplementary data

Supplementary data to this article can be found online at https://doi.org/10.1016/j.intimp.2018.11.013.

References

[1] T.R. Frieden, T.R. Sterling, S.S. Munsiff, C.J. Watt, C. Dye, Tuberculosis, Lancet 362 (9387) (2003) 887–899.
[2] D.F. Warner, A. Koch, V. Mizrahi, Diversity and disease pathogenesis in *Mycobacterium tuberculosis*, Trends Microbiol. 23 (1) (2015) 14–21.
[3] V.H. Ng, J.S. Cox, A.O. Sousa, J.D. MacMicking, J.D. McKinney, Role of KatG catalase-peroxidase in mycobacterial pathogenesis: countering the phagocyte oxidative burst, Mol. Microbiol. 52 (5) (2004) 1291–1302.
[4] J. Korf, A. Stoltz, J. Verschoor, P. De Baetselier, J. Grooten, The *Mycobacterium tuberculosis* cell wall component mycolic acid elicits pathogen-associated host innate immune responses, Eur. J. Immunol. 35 (3) (2005) 890–900.
[5] W. Deng, W. Yang, J. Zeng, A.E. Abdalla, J. Xie, *Mycobacterium tuberculosis* PPE32 promotes cytokines production and host cell apoptosis through caspase cascade accompanying with enhanced ER stress response, Oncotarget (2016).
[6] P. Singh, R.N. Rao, J.R. Reddy, R. Prasad, S.K. Kotturu, S. Ghosh, S. Mukhopadhyay, PE11, a PE/PPE family protein of *Mycobacterium tuberculosis* is involved in cell wall remodeling and virulence, Sci. Rep. 6 (2016) 21624.
[7] S.T. Cole, R. Brosch, J. Parkhill, T. Garnier, C. Churcher, D. Harris, S.V. Gordon, K. Eiglmeier, S. Gas, C.E. Barry III, F. Tekaia, K. Badcock, D. Basham, D. Brown, T. Chillingworth, R. Connor, R. Davies, K. Devlin, T. Feltwell, S. Gentles, N. Hamlin, S. Holroyd, T. Hornsby, K. Jagels, A. Krogh, J. McLean, S. Moule, L. Murphy, K. Oliver, J. Osborne, M.A. Quail, M.A. Rajandream, J. Rogers, S. Rutter, K. Seeger, J. Skelton, R. Squares, S. Squares, J.E. Sulston, K. Taylor, S. Whitehead, B.G. Barrell, Deciphering the biology of *Mycobacterium tuberculosis* from the complete genome sequence, Nature 393 (6685) (1998) 537–544.
[8] N. Casali, L.W. Riley, A phylogenomic analysis of the Actinomycetales mce operons, BMC Genomics 8 (2007) 60.
[9] A. Kumar, A. Chandolia, U. Chaudhry, V. Brahmachari, M. Bose, Comparison of mammalian cell entry operons of mycobacteria: in silico analysis and expression profiling, FEMS Immunol. Med. Microbiol. 43 (2) (2005) 185–195.

[10] A.K. Pandey, C.M. Sassetti, Mycobacterial persistence requires the utilization of host cholesterol, Proc. Natl. Acad. Sci. U. S. A. 105 (11) (2008) 4376–4380.
[11] R. Pasricha, N.K. Saini, N. Rathor, R. Pathak, R. Sinha, M. Varma-Basil, K. Mishra, V. Brahmachari, M. Bose, The *Mycobacterium tuberculosis* recombinant LprN protein of mce4 operon induces Th-1 type response deleterious to protection in mice, Pathog. Dis. 72 (3) (2014) 188–196.
[12] J. Li, Q.Y. Chai, Y. Zhang, B.X. Li, J. Wang, X.B. Qiu, C.H. Liu, *Mycobacterium tuberculosis* Mce3E suppresses host innate immune responses by targeting ERK1/2 signaling, J. Immunol. 194 (8) (2015) 3756–3767.
[13] E. Garcia, M.V. Bianco, M.J. Gravisaco, R.V. Rocha, F.C. Blanco, F. Bigi, Evaluation of *Mycobacterium bovis* double knockout mce2-phoP as candidate vaccine against bovine tuberculosis, Tuberculosis 95 (2) (2015) 186–189.
[14] N. Casali, A.M. White, L.W. Riley, Regulation of the *Mycobacterium tuberculosis* mce1 operon, J. Bacteriol. 188 (2) (2006) 441–449.
[15] C.I. Cheigh, R. Senaratne, Y. Uchida, N. Casali, L.V. Kendall, L.W. Riley, Posttreatment reactivation of tuberculosis in mice caused by *Mycobacterium tuberculosis* disrupted in mce1R, J. Infect. Dis. 202 (5) (2010) 752–759.
[16] K.Y. Dunphy, R.H. Senaratne, M. Masuzawa, L.V. Kendall, L.W. Riley, Attenuation of *Mycobacterium tuberculosis* functionally disrupted in a fatty acyl-coenzyme A synthetase gene fadD5, J. Infect. Dis. 201 (8) (2010) 1232–1239.
[17] S. Chitale, S. Ehrt, I. Kawamura, T. Fujimura, N. Shimono, N. Anand, S. Lu, L. Cohen-Gould, L.W. Riley, Recombinant *Mycobacterium tuberculosis* protein associated with mammalian cell entry, Cell. Microbiol. 3 (4) (2001) 247–254.
[18] S.A. Cantrell, M.D. Leavell, O. Marjanovic, A.T. Iavarone, J.A. Leary, L.W. Riley, Free mycolic acid accumulation in the cell wall of the mce1 operon mutant strain of *Mycobacterium tuberculosis*, J. Microbiol. 51 (5) (2013) 619–626.
[19] M.A. Forrellad, M. McNeil, L. Santangelo Mde, F.C. Blanco, E. Garcia, L.I. Klepp, J. Huff, M. Niederweis, M. Jackson, F. Bigi, Role of the Mce1 transporter in the lipid homeostasis of *Mycobacterium tuberculosis*, Tuberculosis 94 (2) (2014) 170–177.
[20] A. Queiroz, D. Medina-Cleghorn, O. Marjanovic, D.K. Nomura, L.W. Riley, Comparative metabolic profiling of mce1 operon mutant vs wild-type *Mycobacterium tuberculosis* strains, Pathog. Dis. 73 (8) (2015).
[21] N. Shimono, L. Morici, N. Casali, S. Cantrell, B. Sidders, S. Ehrt, L.W. Riley, Hypervirulent mutant of *Mycobacterium tuberculosis* resulting from disruption of the mce1 operon, Proc. Natl. Acad. Sci. U. S. A. 100 (26) (2003) 15918–15923.
[22] R. Stavrum, A.K. Stavrum, H. Valvatne, L.W. Riley, E. Ulvestad, I. Jonassen, J. Assmus, T.M. Doherty, H.M. Grewal, Modulation of transcriptional and inflammatory responses in murine macrophages by the *Mycobacterium tuberculosis* mammalian cell entry (Mce) 1 complex, PLoS One 6 (10) (2011) e26295.
[23] P. Lima, B. Sidders, L. Morici, R. Reader, R. Senaratne, N. Casali, L.W. Riley, Enhanced mortality despite control of lung infection in mice aerogenically infected with a *Mycobacterium tuberculosis* mce1 operon mutant, Microbes Infect. 9 (11) (2007) 1285–1290.
[24] P.C. Sequeira, R.H. Senaratne, L.W. Riley, Inhibition of toll-like receptor 2 (TLR-2)-mediated response in human alveolar epithelial cells by mycolic acids and *Mycobacterium tuberculosis* mce1 operon mutant, Pathog. Dis. 70 (2) (2014) 132–140.
[25] W. Li, X. Fan, Q. Long, L. Xie, J. Xie, *Mycobacterium tuberculosis* effectors involved in host–pathogen interaction revealed by a multiple scales integrative pipeline, Infect. Genet. Evol. 32 (2015) 1–11.
[26] A.K. Pandey, S. Raman, R. Proff, S. Joshi, C.M. Kang, E.J. Rubin, R.N. Husson, C.M. Sassetti, Nitrile-inducible gene expression in mycobacteria, Tuberculosis 89 (1) (2009) 12–16.
[27] W. Deng, J. Zeng, X. Xiang, P. Li, J. Xie, PE11 (Rv1169c) selectively alters fatty acid components of *Mycobacterium smegmatis* and host cell interleukin-6 level accompanied with cell death, Front. Microbiol. 6 (2015) 613.
[28] G. Bashiri, E.F. Perkowski, A.P. Turner, M.E. Feltcher, M. Braunstein, E.N. Baker, Tat-dependent translocation of an F420-binding protein of *Mycobacterium tuberculosis*, PLoS One 7 (10) (2012) e45003.
[29] J. Rengarajan, E. Murphy, A. Park, C.L. Krone, E.C. Hett, B.R. Bloom, L.H. Glimcher, E.J. Rubin, *Mycobacterium tuberculosis* Rv2224c modulates innate immune responses, Proc. Natl. Acad. Sci. U. S. A. 105 (1) (2008) 264–269.
[30] S. Daim, I. Kawamura, K. Tsuchiya, H. Hara, T. Kurenuma, Y. Shen, S.R. Dewamitta, S. Sakai, T. Nomura, H. Qu, M. Mitsuyama, Expression of the *Mycobacterium tuberculosis* PPE37 protein in *Mycobacterium smegmatis* induces low tumour necrosis factor alpha and interleukin 6 production in murine macrophages, J. Med. Microbiol. 60 (Pt 5) (2011) 582–591.
[31] R. Gopalaswamy, S. Narayanan, W.R. Jacobs Jr., Y. Av-Gay, *Mycobacterium smegmatis* biofilm formation and sliding motility are affected by the serine/threonine protein kinase PknF, FEMS Microbiol. Lett. 278 (1) (2008) 121–127.
[32] M. Maya-Hoyos, J. Leguizamon, L. Marino-Ramirez, C.Y. Soto, Sliding motility, biofilm formation, and glycopeptidolipid production in *Mycobacterium colombiense* strains, Biomed. Res. Int. 2015 (2015) 419549.
[33] R. Hussain, A. Ansari, N. Talat, Z. Hasan, G. Dawood, CCL2/MCP-I genotype-phenotype relationship in latent tuberculosis infection, PLoS One 6 (10) (2011) e25803.
[34] Z. Hasan, J.M. Cliff, H.M. Dockrell, B. Jamil, M. Irfan, M. Ashraf, R. Hussain, CCL2 responses to *Mycobacterium tuberculosis* are associated with disease severity in tuberculosis, PLoS One 4 (12) (2009) e8459.
[35] T. Uehata, S. Akira, mRNA degradation by the endoribonuclease Regnase-1/ZC3H12a/MCPIP-1, Biochim. Biophys. Acta 1829 (6–7) (2013) 708–713.
[36] Y.J. Lim, J.A. Choi, J.H. Lee, C.H. Choi, H.J. Kim, C.H. Song, *Mycobacterium tuberculosis* 38-kDa antigen induces endoplasmic reticulum stress-mediated apoptosis via toll-like receptor 2/4, Apoptosis 20 (3) (2015) 358–370.
[37] M.A. Arias, G. Jaramillo, Y.P. Lopez, N. Mejia, C. Mejia, A.E. Pantoja, R.J. Shattock, L.F. Garcia, G.E. Griffin, *Mycobacterium tuberculosis* antigens specifically modulate CCR2 and MCP-1/CCL2 on lymphoid cells from human pulmonary hilar lymph nodes, J. Immunol. 179 (12) (2007) 8381–8391.
[38] Y.J. Lim, J.A. Choi, H.H. Choi, S.N. Cho, H.J. Kim, E.K. Jo, J.K. Park, C.H. Song, Endoplasmic reticulum stress pathway-mediated apoptosis in macrophages contributes to the survival of *Mycobacterium tuberculosis*, PLoS One 6 (12) (2011) e28531.
[39] R.V. Rao, A. Peel, A. Logvinova, G. del Rio, E. Hermel, T. Yokota, P.C. Goldsmith, L.M. Ellerby, H.M. Ellerby, D.E. Bredesen, Coupling endoplasmic reticulum stress to the cell death program: role of the ER chaperone GRP78, FEBS Lett. 514 (2–3) (2002) 122–128.
[40] J. Lehotsky, P. Kaplan, E. Babusikova, A. Strapkova, R. Murin, Molecular pathways of endoplasmic reticulum dysfunctions: possible cause of cell death in the nervous system, Physiol. Res. 52 (3) (2003) 269–274.
[41] A. Roy, P.E. Kolattukudy, Monocyte chemotactic protein-induced protein (MCPIP) promotes inflammatory angiogenesis via sequential induction of oxidative stress, endoplasmic reticulum stress and autophagy, Cell. Signal. 24 (11) (2012) 2123–2131.
[42] K. Wang, J. Niu, H. Kim, P.E. Kolattukudy, Osteoclast precursor differentiation by MCPIP via oxidative stress, endoplasmic reticulum stress, and autophagy, J. Mol. Cell Biol. 3 (6) (2011) 360–368.
[43] H.M. Lee, D.M. Shin, K.K. Kim, J.S. Lee, T.H. Paik, E.K. Jo, Roles of reactive oxygen species in CXCL8 and CCL2 expression in response to the 30-kDa antigen of *Mycobacterium tuberculosis*, J. Clin. Immunol. 29 (1) (2009) 46–56.
[44] C.W. Younce, P.E. Kolattukudy, MCP-1 causes cardiomyoblast death via autophagy resulting from ER stress caused by oxidative stress generated by inducing a novel zinc-finger protein, MCPIP Biochem. J. 426 (1) (2010) 43–53.
[45] P.A. Baeuerle, T. Henkel, Function and activation of NF-kappa B in the immune system, Annu. Rev. Immunol. 12 (1994) 141–179.
[46] M. de la Paz Santangelo, L. Klepp, J. Nunez-Garcia, F.C. Blanco, M. Soria, M.C. Garcia-Pelayo, M.V. Bianco, A.A. Cataldi, P. Golby, M. Jackson, S.V. Gordon, F. Bigi, Mce3R, a TetR-type transcriptional repressor, controls the expression of a regulon involved in lipid metabolism in *Mycobacterium tuberculosis*, Microbiology 155 (Pt 7) (2009) 2245–2255.
[47] O. Marjanovic, T. Miyata, A. Goodridge, L.V. Kendall, L.W. Riley, Mce2 operon mutant strain of *Mycobacterium tuberculosis* is attenuated in C57BL/6 mice, Tuberculosis 90 (1) (2010) 50–56.
[48] I.S. Leal, B. Smedegard, P. Andersen, R. Appelberg, Interleukin-6 and interleukin-12 participate in induction of a type 1 protective T-cell response during vaccination with a tuberculosis subunit vaccine, Infect. Immun. 67 (11) (1999) 5747–5754.
[49] V. Nagabhushanam, A. Solache, L.M. Ting, C.J. Escaron, J.Y. Zhang, J.D. Ernst, Innate inhibition of adaptive immunity: *Mycobacterium tuberculosis*-induced IL-6 inhibits macrophage responses to IFN-gamma, J. Immunol. 171 (9) (2003) 4750–4757.
[50] B.M. Saunders, A.A. Frank, I.M. Orme, A.M. Cooper, Interleukin-6 induces early gamma interferon production in the infected lung but is not required for generation of specific immunity to *Mycobacterium tuberculosis* infection, Infect. Immun. 68 (6) (2000) 3322–3326.
[51] A. Mukherjee, A.R. Khuda-Bukhsh, Quercetin down-regulates IL-6/STAT-3 signals to induce mitochondrial-mediated apoptosis in a nonsmall-cell lung-cancer cell line, A549, J. Pharmacopuncture 18 (1) (2015) 19–26.
[52] L. Song, Y. Li, Y.X. Sun, M. Yu, B.F. Shen, IL-6 inhibits apoptosis of human myeloma cell line XG-7 through activation of JAK/STAT pathway and up-regulation of Mcl-1, Ai Zheng 21 (2) (2002) 113–116.
[53] S.L. Deshmane, S. Kremlev, S. Amini, B.E. Sawaya, Monocyte chemoattractant protein-1 (MCP-1): an overview, J. Interf. Cytokine Res. 29 (6) (2009) 313–326.
[54] J.T. Siveke, A. Hamann, T helper 1 and T helper 2 cells respond differentially to chemokines, J. Immunol. 160 (2) (1998) 550–554.
[55] P.O. Flores-Villanueva, J.A. Ruiz-Morales, C.H. Song, L.M. Flores, E.K. Jo, M. Montano, P.F. Barnes, M. Selman, J. Granados, A functional promoter polymorphism in monocyte chemoattractant protein-1 is associated with increased susceptibility to pulmonary tuberculosis, J. Exp. Med. 202 (12) (2005) 1649–1658.
[56] C.W. Younce, K. Wang, P.E. Kolattukudy, Hyperglycaemia-induced cardiomyocyte death is mediated via MCP-1 production and induction of a novel zinc-finger protein MCPIP, Cardiovasc. Res. 87 (4) (2010) 665–674.
[57] K.H. Kim, Y. Gao, K. Walder, G.R. Collier, J. Skelton, A.H. Kissebah, SEPS1 protects RAW264.7 cells from pharmacological ER stress agent-induced apoptosis, Biochem. Biophys. Res. Commun. 354 (1) (2007) 127–132.